Check for updates

Classification of Fine Particles Using the Hydrodynamic Forces in the Boundary Layer of a Membrane

Philipp Lösch*, Kai Nikolaus, and Sergiy Antonyuk

DOI: 10.1002/cite.201900052

This is an open access article under the terms of the Creative Commons Attribution License, which permits use, distribution and reproduction in any medium, provided the original work is properly cited.

Dedicated to Prof. Dr. techn. Hans-Jörg Bart on the occasion of his 65th birthday

The wet classification of particles < 10 µm is a complex process that has been researched for many years. In this study, the usage of a modified cross-flow filtration process as a classification process was investigated. With this process, particles in a fine micrometer range can be separated from suspensions. The upper particle size is dependent on hydrodynamic forces. The experimental results were compared with different hydrodynamic force models to predict upper size. The influence of the permeate flux and the particle concentration in the feed on the upper particle size is studied.

Keywords: Classification, Cross-flow filtration, Fine particles, Lift force, Wet classification

Received: February 28, 2019; *revised:* July 14, 2019; *accepted:* August 08, 2019

1 Introduction

The application of fine particulate materials (< 10 µm) with a narrow particle size distribution is becoming more common in different products of chemical, food and pharmaceutical industries, such as pigments, polishing compound and active pharmaceutical ingredients. For many such products, it is required that no single coarse particle occurs. While formulation processes like precipitation, crystallization or grinding can generate particle systems smaller than 10 µm, they cannot guarantee that all particles are smaller than a few micrometers and have a narrow particle size distribution. Therefore, a wet classification step after the formulation process is necessary. Wet classification has been a subject of research for many years [1–3]. While conventional wet classification processes like hydro-sieves have upper particle sizes of 20–30 µm [2], hydrocyclones or centrifuges can only separate fine particles in highly concentrated suspensions at great expense. Müller [2] showed that for wet classification processes with particles smaller than 10 µm only setups are capable working by means of sedimentation in the centrifugal field. For this, hydrocyclones with a very small diameter and centrifuges with a very high energy consumption can be used to reach a small cut size. Moreover, the separated particles in a centrifuge are usually compacted which makes their further use ore processing difficult [4]. For a counterflow centrifugal separation, Bickert et al. [5] showed that higher concentrations of the suspension causes bigger particle sizes of the fine fraction. In the work of Konrath [6] cut sizes of 20 nm out of a 200 nm wide distribution were reached with a magnetic beared centrifuge. However, this requires a small throughput and concentration.

For hydrocyclones, Trawinski [7] developed a formula based on Stokes' law and empirical correlation that shows a decrease of the upper particle size with decreasing diameter of the cyclone. For a cut size beneath 1 µm, a hydrocyclone with a diameter smaller than 10 mm will be needed. Neesse [8] showed a classification of particles smaller than 1 µm in a mini-hydrocyclon working at a pressure of 50 bar. However, the small cyclones tend to clog easily. Due to the very small flow rates, they are often operated in parallel.

Mainly, the disadvantages of these conventional processes are a limitation due to the concentration of the suspension and a high energy consumption.

Altmann et al. [9] suggested a new method of wet classification using the cross-flow microfiltration (CMF). They observed a selective particle deposition on a flat membrane and discharged the formed particle layer. Klein [10, 11] designed a test bench and used a back-flush to discharge the particle layer. Meier [12] advanced the previous method using tubular modules. They made qualitative statements about the influence of particle concentration, permeate flux and flow velocity on the upper particle size of the classified product. It was indicated that the upper particle size of

Philipp Lösch, Dr. Kai Nikolaus, Prof. Sergiy Antonyuk
philipp.loesch@mv.uni-kl.de
Technische Universität Kaiserslautern, Institute of Particle Process Engineering, Gottlieb-Daimler-Straße 44, 67663 Kaiserslautern, Germany.

 © 2019 The Authors. Published by WILEY-VCH Verlag GmbH & Co. KGaA, Weinheim

approximately 1 µm can be reached at high flow velocities, low concentrations and low filtration fluxes. Based on these works, a lab-scale setup was designed and constructed. The usability of these effects as classification process was studied.

The present Research Article describes the study of the effects of the ratio between the flow velocity and the permeate flux. Different models of the hydrodynamic forces on a single particle are compared to predict the upper particle size of the classified fraction.

2 Methods and Materials

2.1 Methods

In this work, the CMF is investigated to adapt this method for classification of particles with a size range near to 1 µm. The scheme of the flow channel and the forces on a single particle are shown in Fig. 1. A suspension flows tangentially along the surface of a membrane. The pore size of the membrane is usually smaller than the particle size. Due to a higher pressure on the concentrate side, pure liquid permeates through the membrane (permeate flux). The remaining suspension (retentate) has an increasing concentration. To calculate an upper particle size of the classified particles, Altmann and Ripperger [13] developed a model of the particle deposition, which is based on a hydrodynamic force balance on a single particle. In the boundary layer near to the membrane surface, the movement of the particle orthogonal to the tube flow is determined mainly by drag and lift forces. To avoid the influence of the gravitational force, the membrane is adjusted vertically. The permeate flux creates a drag force on the suspended particles which transports them towards the membrane surface. The low permeate flow velocity through the pores causes a small particle Reynolds number ($5 \cdot 10^{-7} < Re < 5 \cdot 10^{-4}$). Under these conditions, the drag force F_D can be estimated with the Stokes' law as

$$F_D = 3\pi\eta x(v_F - v_P) \tag{1}$$

with the particle diameter x, the dynamic viscosity η, the permeate flux v_F and the velocity of the particle v_P.

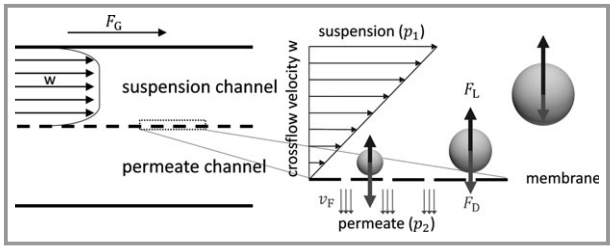

Figure 1. Scheme of the forces on a single particle in the laminar boundary flow at the membrane surface.

The velocity gradient in the boundary layer of the crossflow creates a lift force on the particles, which transports them back into the bulk flow. In the past, many theoretical and experimental investigations were performed in order to describe this lift force. First, Segré, and Silberberg [14] described the effect of a radial particle displacement in a poiseuille flow. In the experimental study, they observed that after a short inflow distance, the particles concentrating in a stationary distribution across the tube radius. Their suggest for a drag force on a single spherical particle is dependent on the square of the mean flow velocity and the particle size in the fourth power. In a full report at a later time [15, 16] they described the measuring method and their results. They revoked their previous assumption and determined the influence of the particle size with the third power. To describe these experimental results physically, Saffman [17] developed based on a theoretical investigation the following correlation:

$$F_{L,Saffman} = \frac{0.807 x^3 \tau_w^{1.5} \rho^{0.5}}{\eta} \tag{2}$$

with the density of the fluid ρ and the wall shear stress τ_w, which is defined as:

$$\tau_w = \frac{\lambda}{8} \rho w^2 \tag{3}$$

where the mean velocity of the flow is and the parameter describes the roughness of the membrane.

Rubin [18] suggested a variation of the Saffman approach, which differs only in the empirical coefficient which he determined from experiments. He investigated the drag and lift coefficient of a stationary spherical particle in a laminar boundary layer of a tube.

$$F_{L,Rubin} = \frac{0.761 x^3 \tau_w^{1.5} \rho^{0.5}}{\eta} \tag{4}$$

While [16–18] tried to estimate the shear flow of a poiseuille flow, the theoretical work of Leighton and Acrivos [19] uses a numerically evaluated correlation for the lift force on a sphere touching a plane in the presence of a simple shear flow:

$$F_{L,Leighton} = \frac{0.576 x^4 \tau_w^2 \rho}{\eta} \tag{5}$$

The lift and the drag forces are variously dependent on the particle size. By regulating the flow velocity and permeate flux, an equilibrium of forces at one particle size can be adjusted by considering the lateral particle velocity to be zero [20]. In this case, the drag force in Eq. (1) equals the lift force. Using Eq. (4) for the lift force, an upper particle size in Eq. (6) can be found, which describes the upper particle size of the classified fraction deposited on the membrane surface.

 © 2019 The Authors. Published by WILEY-VCH Verlag GmbH & Co. KGaA, Weinheim

15222640, 2019, 11, Downloaded from https://onlinelibrary.wiley.com/doi/10.1002/cite.201900052 by Rheinland-Pfälzische Technische Universität Kaiserslautern-Landau, Wiley Online Library on [04/04/2024]. See the Terms and Conditions (https://onlinelibrary.wiley.com/terms-and-conditions) on Wiley Online Library for rules of use; OA articles are governed by the applicable Creative Commons License

$$x_{max} = \sqrt{\frac{v_F \eta^2}{0.00357 \lambda^{1.5} \rho^2 w^3}} \quad (6)$$

The drag force dominates for smaller sizes of particles, which will be deposited on the membrane. At a particle size bigger than x_{max}, the lift force will be dominant and the particle will be transported from the boundary layer back into the bulk flow. For a particular flow velocity, a suiting permeate flux can be calculated. To predict the upper particle size for the classified fraction, the experimental results have to be compared with the different models of the lift force.

2.2 Setup and Parameters of the Experiments

An experimental setup in lab-scale (Fig. 2) was designed and used for the performed experiments. It contains a tube module with tubular polypropylene (PP) membranes, which exhibit a good resistance against back flushing, which is needed for the resuspending of the particles. The nominal pore size of the used membranes is 0.2 µm. By changing the self-constructed membrane module, the effective membrane area can be adjusted with different membrane elements between 0.008 and 0.104 m^2. In this work, 10 membranes with a diameter of 5.5 mm and an area of 0.104 m^2 was used. The membranes are arranged in a circular path in order to ensure a uniform flow in all tubular membranes. To prevent an influence of the inflow, the filter area of the entry of the membranes were closed. The open filtration area starts with a uniform flow in the membrane.

In order to prevent sedimentation in the membranes, the tube module was implemented vertically.

The particles are suspended with a stirrer in the suspension tank with a regulated temperature. A speed-controlled pump (1) produces a defined constant flow through the membrane module which is indicated by a magnetic inductive flow meter (2). A flow velocity up to 3 m s^{-1} is possible. By modulating the transmembrane pressure (TMP) with a membrane valve (3), the permeate flux can be adjusted and measured by a second magnetic inductive flow meter (7). The TMP is calculated with the measured pressure at the inlet (4) and outlet (5) of the membrane module and the pressure of the flux (6). After an initial period of 15 min to ensure a dispersion of the particles in the system, the TMP has to be increased in stages. This prevents a high flux at the beginning of the filtration and thus particles larger than the required upper particle size. During the classification process the TMP was also further increased to prevent a decreasing permeate flux caused by an increasing cake resistance. If the TMP exceeds 2 bar, or if no temporal change of the TMP is noticeable, the deposition will be stopped.

After rinsing the system with filtered liquid, the membranes are backflushed and the classified fraction is

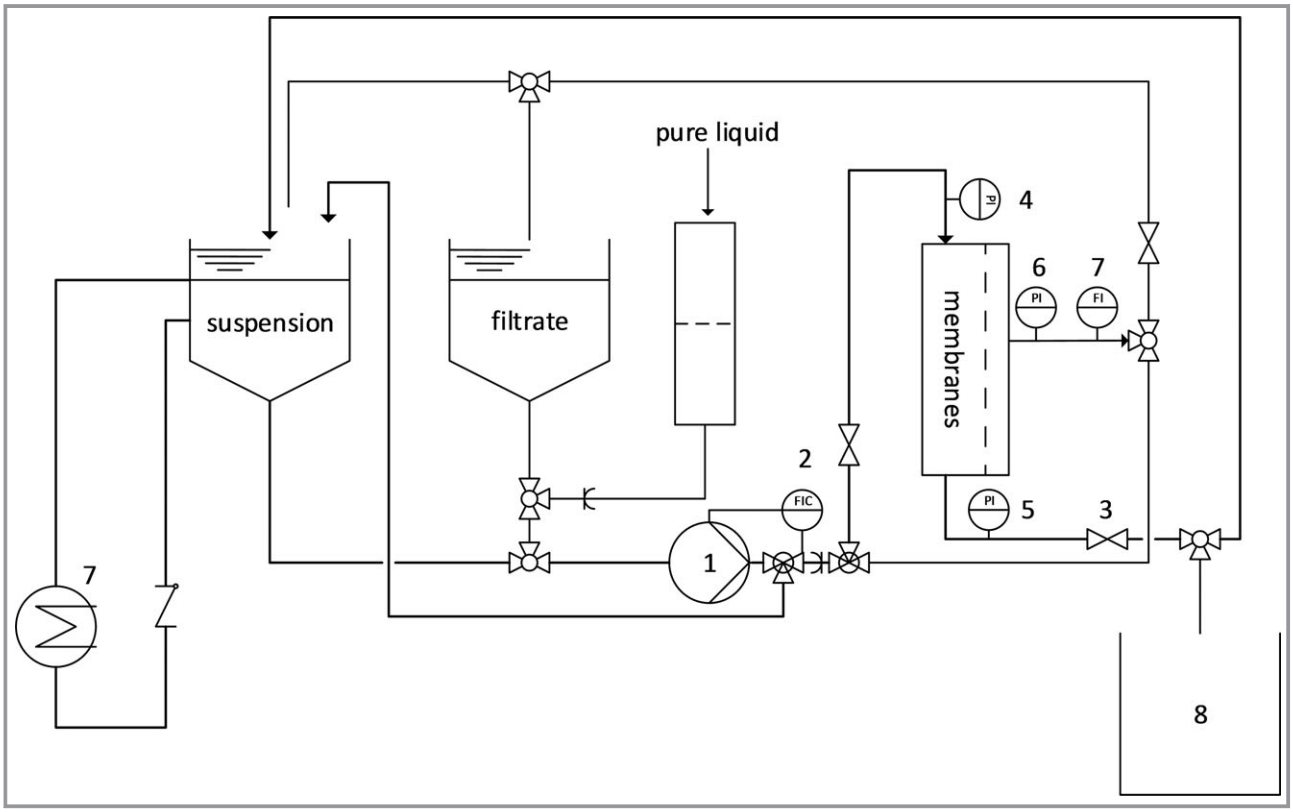

Figure 2. Schematic representation of the experimental setup.

 © 2019 The Authors. Published by WILEY-VCH Verlag GmbH & Co. KGaA, Weinheim

15222640, 2019, 11, Downloaded from https://onlinelibrary.wiley.com/doi/10.1002/cite.201900052 by Rheinland-Pfälzische Technische Universität Kaiserslautern-Landau, Wiley Online Library on [04/04/2024]. See the Terms and Conditions (https://onlinelibrary.wiley.com/terms-and-conditions) on Wiley Online Library for rules of use; OA articles are governed by the applicable Creative Commons License

discharged from the system and resuspended in an additional tank (8).

With the developed setup, a parameter study on the influence of the mean velocity of the cross-flow on the upper particle size and the selectivity was performed. The flow velocity was variied between 0.5 and 1.05 m s^{-1}. After resuspending the classified fraction, the permeate flux of the separation equilibrium can be adjusted again, to classify encore small particles. The particle size distribution of the resuspended and remaining fraction was than analyzed.

2.3 Materials

To proof the independence of the process efficiency from the particle size distribution and their width, suspensions with calcium carbonate ($CaCO_3$, CALCIT MS 70 F, Calcitwerk Schön & Hippelein GmbH & Co. KG, ρ_s = 2700 kg m^{-3}) and alumina (Al_2O_3, CT 3000 LS SG, ALMATIS B.V., ρ_s = 3950 kg m^{-3}) were used for the experiments. The particle size distributions (Fig. 3) were measured in liquid phase (water) by a static light scattering device (HORIBA LA-950, Retsch). The $CaCO_3$ particles show a very wide distribution, from 0.1 µm to 60 µm. The Al_2O_3 suspension is bimodal distributed in the range of 0.01–4 µm. To verify the measured particle size distributions, images with a scanning electron microscope (Phenom G2) were made (Fig. 4).

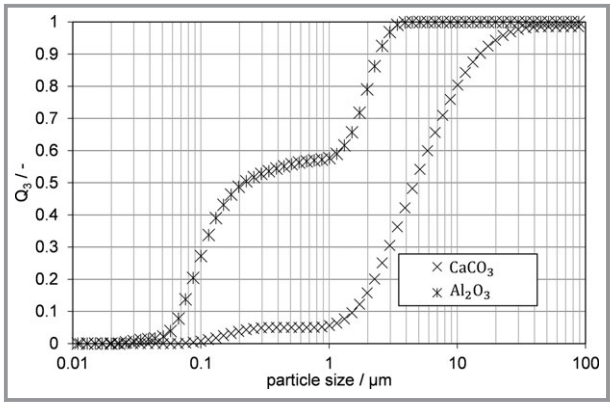

Figure 3. Particle size distribution of initial $CaCO_3$ and Al_2O_3.

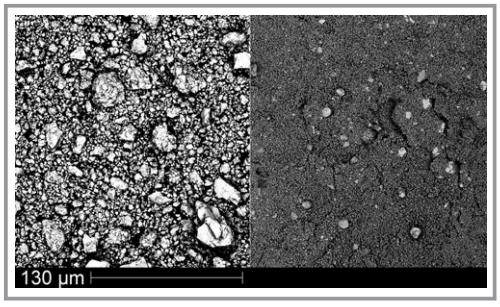

Figure 4. Images of the initial fraction of $CaCO_3$ (left) and Al_2O_3 (right) obtained by a scanning electron microscope.

3 Results and Discussions

3.1 Influence of the Permeate Flux

In order to investigate the influence of the permeate flux, experiments with $CaCO_3$ particles were performed. The permeate fluxes were adjusted successively to 167, 396, and 619 L $m^{-2}h^{-1}$. The flow velocity was 0.76 m s^{-1} and the volume concentration was φ_s = 0.116 %. Fig. 5 shows the particle size distributions of the feed and of the classified fractions. Following Eq. (6) smaller flux rates at the same flow velocity lead to smaller upper particle sizes. The experimental results confirm the decreasing mean particle size of the fine fraction for smaller permeate fluxes. Furthermore, the amount of particles smaller than 2 µm decreases with higher permeate fluxes respectively. This indicates the withdrawal of finest particles out of the suspension with each classification step. For analysis of the separation efficiency, especially to trace oversized particles, scanning electron microscope images of the classified fraction were made (Fig. 6). The separation of the big particles is visible and at a higher flux rate, the upper particle size of the classified fraction increased.

With the different models of the lift force (Eqs. (2), (4), and (5)), the drag force (Eq. (1)) and the parameters in Tab. 1, different upper particle sizes can be calculated (Tab. 2). The comparison of the different approaches in

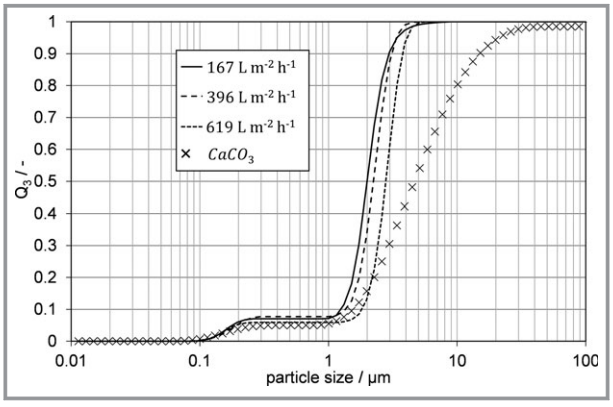

Figure 5. Particle size distribution of the feed and the classified fraction of $CaCO_3$.

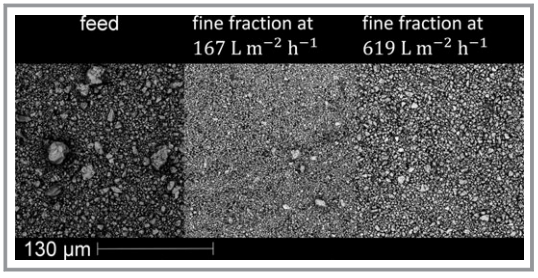

Figure 6. Images of the feed and classified fraction of $CaCO_3$ made by a scanning electron microscope.

 © 2019 The Authors. Published by WILEY-VCH Verlag GmbH & Co. KGaA, Weinheim

15222640, 2019, 11, Downloaded from https://onlinelibrary.wiley.com/doi/10.1002/cite.201900052 by Rheinland-Pfälzische Technische Universität Kaiserslautern-Landau, Wiley Online Library on [04/04/2024]. See the Terms and Conditions (https://onlinelibrary.wiley.com/terms-and-conditions) on Wiley Online Library for rules of use; OA articles are governed by the applicable Creative Commons License

Table 1. Parameters for the different lift force models of $CaCO_3$.

w [m s^{-1}]	0.76
v_F [L m^{-2}h^{-1}]	167
η [Pa s]	0.001
ρ [kg m^{-3}]	1000
λ [–]	0.039
φ_s [%]	0.116

relation to the drag force depending on the particle size is shown in Fig. 7. If the lift force is bigger than the drag force, the particles should be uplifted into the bulk flow.

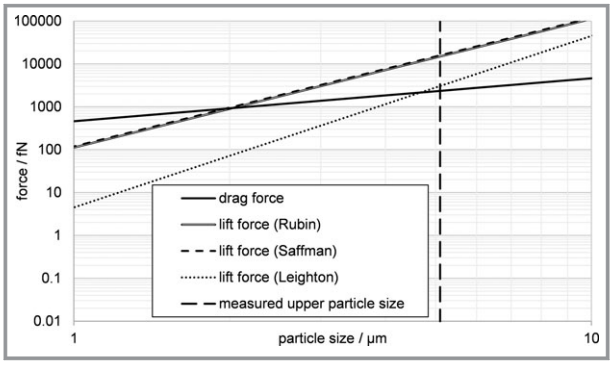

Figure 7. Equilibrium of forces with different lift force and drag force models for the data in Tab. 1.

By comparing the results of the measured particle size distributions with the different models of the lift force (Tab. 2 and Fig. 7), the lift force model of Leighton shows the best prediction of the upper particle size.

3.2 Influence of the Concentration

To consider the differences between models and the experimental results, the concentration of the suspension is regarded. The Stokes-Equation is valid only for very low particle concentration without particle interactions. A correction factor for high concentration is required.

$$F_{D,\varphi_s} = 3\pi\eta x v_F \xi(\varphi_s) \tag{7}$$

Brinkmann [21] suggested a correction factor for monodisperse particles which only depends on the volume concentration.

$$\xi(\varphi_s) = \frac{4 + 3\varphi_s + 3\sqrt{8\varphi_s - 3\varphi_s^2}}{(2 - 3\varphi_s)^2} \tag{8}$$

The correction factor of Brinkmann leads to a small positive linear shift of the drag force in the force-particle size plot (Fig. 8).

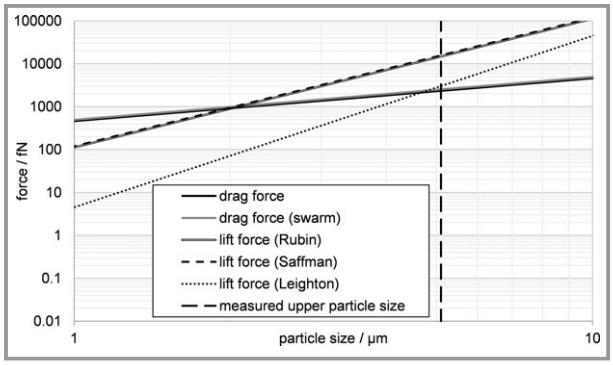

Figure 8. Equilibrium of lift and drag forces with the influence of the concentration.

For the concentration of φ_s = 0.116 %, the upper particle sizes are shown in Tab. 2. Due to the consideration of the swarm influence, the measured upper particle size becomes closer to the model of Leighton. Considering this, the upper particle size is defined as:

$$x_{max,Leighton,Brinkmann} = \sqrt{\frac{1047 v_F \eta^3 \xi(\varphi_s)}{\lambda^2 \rho^3 w^4}} \tag{9}$$

Table 2. Predicted and measured upper particle size at a flux rate of 167, 396, and 619 L m^{-2}h^{-1}.

	167 L m^{-2}h^{-1}		396 L m^{-2}h^{-1}		619 L m^{-2}h^{-1}	
	Single particle model	Influence of concentration	Single particle model	Influence of concentration	Single particle model	Influence of concentration
Predicted upper particle size (Saffman) [µm]	1.94	2.01	2.91	3.02	3.63	3.77
Predicted upper particle size (Rubin) [µm]	2.00	2.08	2.99	3.11	3.75	3.89
Predicted upper particle size (Leighton) [µm]	4.62	4.75	6.06	6.21	7.03	7.21
Measured upper particle size (x_{99}) [µm]	5.10	5.10	3.90	3.90	5.87	5.87

 © 2019 The Authors. Published by WILEY-VCH Verlag GmbH & Co. KGaA, Weinheim

15222640, 2019, 11, Downloaded from https://onlinelibrary.wiley.com/doi/10.1002/cite.201900052 by Rheinland-Pfälzische Technische Universität Kaiserslautern-Landau, Wiley Online Library on [04/04/2024]. See the Terms and Conditions (https://onlinelibrary.wiley.com/terms-and-conditions) on Wiley Online Library for rules of use; OA articles are governed by the applicable Creative Commons License

3.3 Investigation of the Efficiency

In order to investigate the decreasing of finest particles in the retentate of the classification process, an experiment with $CaCO_3$ was performed. The parameters are shown in Tab. 3. For this investigation, three classification processes of approximately 20 min each were performed, using the retentate of the previous classification step respectively. The classification is performed at lower flow velocity and a higher permeate flux as in the first experiment of Fig. 5.

Table 3. Parameters of the experimental investigation of the efficiency.

w [m s^{-1}]	0.43
v_F [L m^{-2}h^{-1}]	200
η [Pa s]	0.001
ρ [kg m^3]	1000
λ [–]	0.039
φ_s [%]	0.116

The distributions of the suspension, the classified fractions and the retentate are displayed in Fig. 9. A classification of particles < 8 µm is recognizable. The particle size distribution of the three classified fractions are similar to each other. In the retentate, the proportion of smaller particles is decreased compared to the initial distribution. But there are still fine particles left. A comparison with the predicted upper particle size is shown in Tab. 4. The upper particle size calculated with Eq. (9) has the best agreement with the experimental results.

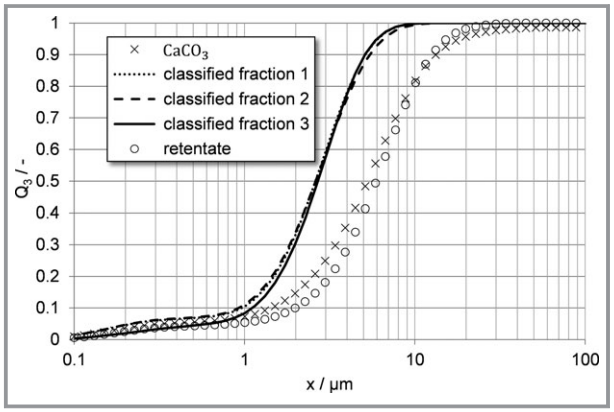

Figure 9. Particle size distribution of the feed, the classified fraction of $CaCO_3$ and the retentate.

3.4 Influence of a Narrow Particle Size Distribution

To study the classification of a suspension with smaller particle having a narrow size distribution, further experiments with Al_2O_3 powder are performed. An flow velocity of 1.05 m s^{-1} and a permeate flux of 115 L m^{-2}h^{-1} were adjusted. The volume concentration was φ_s = 0.116 %. The permeate flux was calculated with Eq. (9) to adjust an upper particle size of 2.75 µm. At this flow velocity, it was the smallest possible flux at this setup. Fig. 10 shows the results of a classification of Al_2O_3 particles. The classified fraction is smaller than 2 µm. Almost 85 mass % of the cumulative particle size distribution is below than 1 µm. In Tab. 5, the comparison with the predicted upper particle size is shown.

In this case, the models of Saffman and Rubin underestimate and the model of Leighton overestimates the reached upper particle size.

Table 4. Predicted and measured upper particle size at a flux rate of 200 L m^{-2}h^{-1}.

Fraction	1	2	3
Predicted upper particle size (Saffman) [µm]		4.51	
Predicted upper particle size (Rubin) [µm]		4.65	
Predicted upper particle size (Leighton) [µm]		9.58	
Measured upper particle size (x_{99}) [µm]	8.81	10.10	7.70

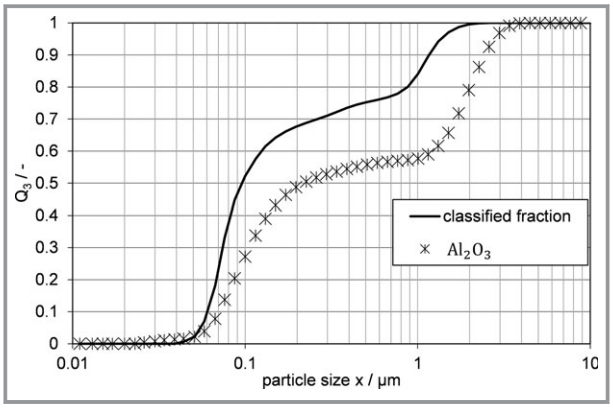

Figure 10. Particle size distribution of the feed and the classified fraction of Al_2O_3.

Table 5. Predicted and measured upper particle size of Al_2O_3 at a flux rate of 115 L m^{-2}h^{-1} with consideration of the concentration influence.

Predicted upper particle size (Saffman) [µm]	1.01
Predicted upper particle size (Rubin) [µm]	1.04
Predicted upper particle size (Leighton) [µm]	2.75
Measured upper particle size (x_{99}) [µm]	2.27

4 Conclusion

In the present work, a possible prediction of the upper particle size of a new wet classification process based on the cross-flow filtration was studied. For the investigation of

 © 2019 The Authors. Published by WILEY-VCH Verlag GmbH & Co. KGaA, Weinheim

15222640, 2019, 11, Downloaded from https://onlinelibrary.wiley.com/doi/10.1002/cite.201900052 by Rheinland-Pfälzische Technische Universität Kaiserslautern-Landau, Wiley Online Library on [04/04/2024]. See the Terms and Conditions (https://onlinelibrary.wiley.com/terms-and-conditions) on Wiley Online Library for rules of use; OA articles are governed by the applicable Creative Commons License

the process parameters, a test lab-scale setup was designed. Two different particle systems ($CaCO_3$ and Al_2O_3) were used for the investigation of the classification. The measured particle size distributions show a successfully classification of finer fraction. Images of the classified fraction with a scanning electron microscope showing a very small and narrow particle size distribution with only few bigger particles. The influence of the width of the particle size distribution seems negligible. The upper particle size was compared with different models of the hydrodynamic forces. By consideration of the concentration in the model of the particle deposition, the experimental data can get closer to the requested separation size. In this study, the influence of the concentration was small, but with higher concentration, the influence will increase. Furthermore, the influence of the particle concentration on the lift force has to be investigated. An additional influence on the hydrodynamic forces is the particle shape, because all hydrodynamic models consider spherical particles. By using the approach of lift force models, a modified cross-flow setup can be used to classify particles < 5 µm with simple methods.

These investigations were financially supported by the German Research Foundation: SPP 2045 MehrDimPart, project AN 782/9-1 "Multidimensional fractionation of finely dispersed particles using cross-flow filtration with superimposed electric field", which the authors gratefully acknowledge.

Symbols used

F_D	[N]	drag force
F_L	[N]	lift force
x	[µm]	particle diameter
v	[m s^{-1}]	velocity
w	[m s^{-1}]	flow velocity

Greek symbols

η	[Pa s]	dynamic viscosity
λ	[–]	surface roughness
ξ	[–]	factor for concentration
ρ	[kg m^{-3}]	density
τ_w	[N m^{-2}]	wall shear stress
φ_s	[%]	volume concentration

Subscripts

F	fluid
P	particle

References

[1] K. G. H. Heiskanen, *Int. J. Miner. Process.* **1996**, *44–45*, 29–42.
[2] F. Müller, *Chem. Eng. Technol.* **2010**, *33 (9)*, 1419–1426. DOI: https://doi.org/10.1002/ceat.200900540
[3] H. Schubert, *Part. Sci. Technol.* **1983**, *1 (4)*, 393–408. DOI: https://doi.org/10.1080/02726358308906384
[4] J. Schmidt, *Wirbelschichtklassierung von Feinstkornsuspensionen im Zentrifugalfeld*, Books on Demand **2005**.
[5] G. Bickert, W. Stahl, R. Bartsch, F. Müller, *Chem. Ing. Tech.* **1993**, *65 (7)*, 822–825.
[6] M. Konrath, J. Gorenflo, N. Hübner, H. Nirschl, *Chem. Eng. Sci.* **2016**, *147*, 65–73. DOI: https://doi.org/10.1016/j.ces.2016.03.025
[7] H. Trawinski, *Chem. Ing. Tech.* **1958**, *30 (2)*, 85–95. DOI: https://doi.org/10.1002/cite.330300206
[8] T. Neesse, J. Dueck, H. Schwemmer, M. Farghaly, *Minerals Engineering* **2015**, *71*, 85–88. DOI: https://doi.org/10.1016/j.mineng.2014.10.017
[9] J. Altmann, S. Ripperger, *Chem. Ing. Tech.* **1998**, *70 (11)*, 1402–1406. DOI: https://doi.org/10.1002/cite.330701109
[10] G.-M. Klein, Untersuchungen zum Deckschichtaufbau bei Querstrom-Mikrofiltration polydisperser Suspensionen unter definierten Strömungsbedingungen, *Dissertation*, Universität Stuttgart **1999**.
[11] G.-M. Klein, V. Kottke, *EP0874692B1*, **2003**.
[12] J. Meier, G.-M. Klein, V. Kottke, *Sep. Purif. Technol.* **2002**, *26 (1)*, 43–50. DOI: https://doi.org/10.1016/S1383-5866(01)00115-0
[13] J. Altmann, S. Ripperger, *J. Membr. Sci.* **1997**, *124 (1)*, 119–128. DOI: https://doi.org/10.1016/S0376-7388(96)00235-9
[14] G. Segré, A. Silberberg, *Nature* **1961**, *189 (4760)*, 209. DOI: https://doi.org/10.1038/189209a0
[15] G. Segré, A. Silberberg, *J. Fluid Mech.* **1962**, *14 (1)*, 115–135. DOI: https://doi.org/10.1017/S002211206200110X
[16] G. Segré, A. Silberberg, *J. Fluid Mech.* **1962**, *14 (1)*, 136–157. DOI: https://doi.org/10.1017/S0022112062001111
[17] P. G. Saffman, *J. Fluid Mech.* **1965**, *22-2*, 385–400.
[18] G. Rubin, Widerstands- und Auftriebsbeiwerte von ruhenden, kugelförmigen Partikeln in stationären, wandnahen laminaren Grenzschichten, *Dissertation*, Universität Karlsruhe (TH) **1977**.
[19] D. Leighton, A. Acrivos, *Z. Angew. Math. Phys.* **1985**, *36 (1)*, 174–178. DOI: https://doi.org/10.1007/BF00949042
[20] M. T. Nguyen, Deckschichtbildung in Kapillarmembranen bei der Querstrom-Mikrofiltration und ihre Beeinflussung durch polymere Flockungsmittel, *Dissertation*, Technische Universität Dresden **2004**.
[21] H. C. Brinkman, *Appl. Sci. Res.* **1949**, *1 (1)*, 1045. DOI: https://doi.org/10.1007/BF02120313

 © 2019 The Authors. Published by WILEY-VCH Verlag GmbH & Co. KGaA, Weinheim

15222640, 2019, 11, Downloaded from https://onlinelibrary.wiley.com/doi/10.1002/cite.201900052 by Rheinland-Pfälzische Technische Universität Kaiserslautern-Landau, Wiley Online Library on [04/04/2024]. See the Terms and Conditions (https://onlinelibrary.wiley.com/terms-and-conditions) on Wiley Online Library for rules of use; OA articles are governed by the applicable Creative Commons License